RSC Advances

ROYAL SOCIETY OF CHEMISTRY

www.rsc.org/advances

Journal Name

ARTICLE TYPE

A novel sulfur/carbon composite for low cost lithium-sulfur batteries with high cycling stability

Yanhong Yin[a,b,c], **Chao Ma**[a,b,c], **Zhaoxia Cao**[a,b,c], **Zhixian Sun**[a,b,c], **Yujie Jia**[a,b,c] **and Shuting Yang**[a,b,c] *

Lithium sulfur (Li-S) battery is a promising electrochemical system for the next generation high density rechargeable battery having a theoretical energy density of ~2600 Wh/kg. In spite of the intrinsic advantages, Li-S batteries currently are confronted with a variety of problems such as low specific capacity and short cycle life. In this work, a novel sulfur/carbon composite was prepared using coconut 10 shell carbon as raw materials for Li-S batteries. The structure of the composite could accommodate the volume expansion of sulfur particles and trap the dissolved polysulfide produced during the electrochemical reaction. Therefore, the composite based cell demonstrates a high initial capacity of 878 mAh/g at a rate of 0.1 *C*, and excellent cycling stability, in which a reversible capacity of 774 mAh/g was maintained even after 50 cycles.

15

Introduction

Sulfur, one of the most abundant elements on the earth, is of low cost and environmental benign when used as the cathode material. Therefore, the lithium/sulfur battery is a promising 20 electrochemical system having a high theoretical capacity of 1675 mAh/g for the next generation high density rechargeable battery.[1-3] In the past two decades, the practical development of the lithium/sulfur battery is rather limited, because the low utilization of sulfur active material and its poor cycle stability.[1] 25 The disadvantages are that the highly insulating nature of sulfur (5×10^{-30} S/cm at 25 ℃), and lithium polysulfides as intermediate generated products, are easily dissolvable, during the electrochemical reduction reaction process.[3]

Recently, different porous carbon-based sulfur composites have 30 been proved to be feasible in solving the aforementioned problems because of porous carbon's high electronic conductivity and electrochemical affinity for sulfur.[4, 5] Carbon substrates with different pore structure can offer different advantages for sulfur–carbon cathode materials, such as activated carbon, microporous 35 carbon, carbon nanotubes, graphene sheets and so on.[5] Carbon spheres can encapsulate sulfur, but the total pore volume needs to be increased to enhance the sulfur loading.[6, 7] Porous carbon nanofibers and hollow carbon nanofibers or nanotubes are also good substrates to be impregnated with sulfur.[8-13] Graphene oxide 40 has also been used, but the graphene/sulfur composite may need further treatment for immobilizing the intermediate polysulfides.[14-16] Mesoporous hollow carbon capsules were synthesized to trap and sequester elemental sulfur in its interior and porous shells. This unique structure could reduce the

45 dissolution of polysuldes and provide channels for electrons diffusion, which leads to high cycling stability.[17] Some mesoporous carbons with highly ordered pores were also reported with high capacities and cycling performance due to their unique pore structures.[18-20] Although these carbon-based sulfur 50 composites demonstrate outstanding enhancement in Li-S battery performance, facile and low cost fabrication techniques are still desired for industrial scale production.

Fig. 1 Schematic of coconut shell carbon for improved matrix 55 structures.

Herein, we employed a low cost carbon-coconut shell carbon (CSC) and a facile producing technique to prepare the cathode material for Li-Sulfur batteries. As it is displayed in Fig. 1, the synthesis of the CSC experienced a two-step calcination process. 60 As it is displayed in Fig. 1, coconut shells were firstly calcinated under N_2 atmosphere. Then, the intermediate product was mixed with KOH, and calcinated again and washed with acid and distilled water to final yield the CSC. The as-prepared sulfur/coconut shell carbon (CSC@S) exhibited a high reversible 65 capacity of 878 mAh/g and a long cycling performance. The improved cycling stability would be attributed to the reduced sulfur size and the enhanced electric contact provided by the increased confinement of sulfur in the carbon matrix.[21]

Experimental

The coconut shells were dried 24 hours in Stand-Drying and Air Circulation Oven before used. Then the dried coconut shells were pre-carbonized at 600 ℃ for 6 hours with a heating rate of 5 ℃ /min in a in a box-type furnace under N_2 atmosphere. After

5 cooling, grinding and screening, the resulting coconut shell carbon, was sieved and mixed with KOH (mass ratio 1:1) under a following N_2 atmosphere at 900 ℃ for 2 hours with a heating rate of 5 ℃ /min in a box-type furnace.[22] After cooling down to the room temperature, it was washed by diluted HNO_3 and

10 neutralized by distilled water. Finally, the resulting products were dried at 80 ℃ for 24 hours. The mixture of the as-prepared coconut shell carbon and sulfur (sublimed sulfur, with a purity of > 99.995%) were thoroughly mixed according to mass ratios (4:6) of sulfur and carbon in an agate mortar to yield a black mixture.

15 The mixture was then sealed in an air-free glass container and heated at 155 ℃ for 6 hours to obtain sulfur/coconut shell carbon composite (CSC@S). A possible mechanism should be that within the air-free container, the capillary force of the meso/micropores can be enhanced by at the low pressure

20 conditions, which makes it easier for the penetration of the melt sulfur into the pores. Therefore, the composite structure can be easily obtained.

The specific surface area was measured by the Brunauer-Emmet-Teller method (BET, Tristar-Ⅱ, Micromeritics). The crystalline

25 phases of the samples were determined by X-ray diffraction (XRD, Bruker AXS D8) analysis equipped with Cu-Kα radiation. The sample surface morphology was examined by field emission scanning electron microscopy (FESEM, SU-8010, HITACHI).

For electrochemical evaluation, the CSC@S working electrodes

30 were made by mixing the active material, Super P and PVDF with NMP (N-methyl-2-pyrrolidine) as solvent at same ratio (80:10:10). The separator was a polypropylene membrane with micropores (Celgard 2400). Lithium metal was used as counter and reference electrode. The electrolyte used was 1 M $LiPF_6$ in a

35 mixture of ethylene carbonate (EC) and diethyl carbonate (DEC) (1:1 volume).

Galvanostatic charge-discharge experiment data were collected using LAND Cell test system (CT2001A, Wuhan, China). A.C. impedance and cyclic voltammetry (CV) measurements were

40 conducted with a CHI660B electrochemical workstation using fresh cells at open potential. A.C. impedance spectra were measured at 10 mV amplitude with a frequency range from 0.1 Hz to100 KHz. The CV measurement was performed in the range of 1.2-2.8 V at a scanning rate of 0.05 mV/s.

Results and discussion

45
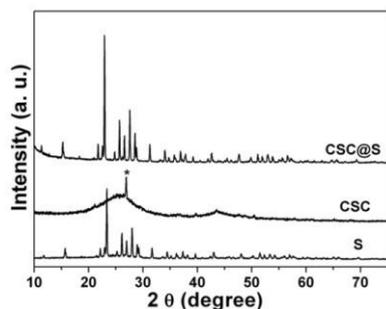
Fig. 2 X-ray diffraction patterns of S, CSC and s CSC@S.

Fig. 2 shows the XRD patterns of the pristine sulfur powders and the as-prepared CSC@S composites, respectively. All diffraction

50 peaks of sulfur match very well with the standard diffraction lines of sulfur (JCPDS card NO. 08-0247). For sulfur/carbon composites, the XRD pattern consists of diffraction peaks of sulfur and a broad diffraction peak at 25°, which corresponds to amorphous carbon in the composite. In addition, the peak located

55 at 27° (marked with star) was also observed, corresponding to the diffraction peak of silica (JCPDS card NO. 46-1045). The existence of silica could result from the Si element contained in the coconut shell raw materials. Compare with the XRD pattern of elemental sulfur, the XRD spectra of the CSC@S composite

60 exhibit the peak of sulfur, demonstrating that the sulfur was decorated in the CSC, which could permit the high electron conductivity.
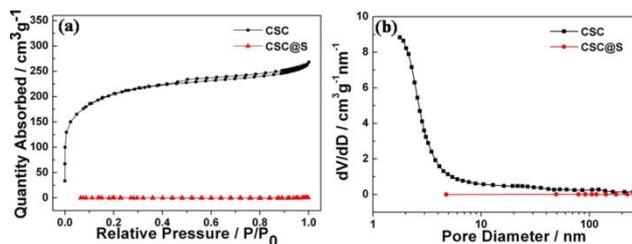
Fig. 3 a) N_2 sorption isotherm and b) pore size distribution of the

65 composite cathode containing coconut shell carbon.

To illustrate the porous structure of the CSC, we measured the nitrogen adsorption–desorption isotherm (Fig. 3a) and the corresponding density functional theory pore size distribution curve (Fig. 3b) at 77 K. The Brunauer-Emmett-Teller (BET)

70 surface area and pore volume are 677 m^2/g and 0.29 cm^3/g, respectively, with cumulative volume of pores diameter between 1.7 nm and 300 nm. From the t-Plot report, micropore area and micropore volume are 237 m^2/g and 0.07 cm^3/g. It can be seen in Fig. 3b that the carbon also has a hierarchical pore size

75 distribution, mainly in two regions: 1.7~2.0 nm and 2.1~50 nm, representing two level abundant micropores and small mesopores. The microporous channels in the composite can restrict the diffusion of the polysulfides during the cycling.
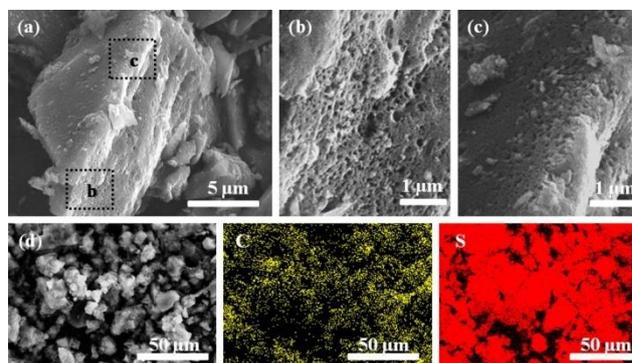
80 **Fig. 4** SEM images of a-c) the CSC, d) the CSC@S composites, elemental mapping of carbon and sulfur of CSC@S before testing.

The SEM images of the CSC are show in Fig. 4a-c. The particle size is about several tens of micrometers. From the magnified images of the particle surface, it is obviously that the as-prepared

85 CSC is rich in pores with diameter from several tens to hundreds

of nanometers. The CSC has a porous structure which agrees with the N_2 adsorption/desorption isotherms (Fig. 3a). The carbon and sulfur elemental mapping clearly demonstrate that sulfur is homogeneously distributed in the matrix of CSC, with the sulfur

5 (red) map matching well with the carbon (yellow) map (Fig. 4d). As it is displayed in Fig. 5a, the CSC@S composite shows a high initial capacity of 878 mAh/g at a rate of 0.1 C (1 C =1675 mA/g) and the reversible capacity remains high at up to 774 mAh/g even after 50 cycles. As a comparison, the cathode derived from

10 activated carbon-sulfur composite shows very poor cyclability, and the capacity drops to below 400 mAh/g after 50 cycles.
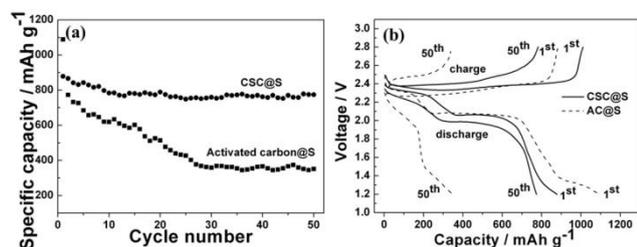
Fig. 5 a) Cycling stability of the CSC@S cathode at a rate of 0.1 C for 50 cycles, b) galvanostatic discharge/charge profiles at 0.1 C.

15 In order to further investigate the electrochemical performance of the CSC@S composite, galvanostatic cycling performance was studied. Fig. 5b displays the typical discharge/charge profiles for the first and 50th cycles at the rate of 0.1 C between 1.2 and 2.8 V. Two plateaus are presented in the discharge profile of the cell: a

20 short higher potential plateau at about 2.3 V and the other prolonged lower potential plateau at about 2.1 V. The 2.4 V plateau is ascribed to the transformation from sulfur to the higher-order lithium polysulfides, which are soluble in the liquid electrolyte. Furthermore, at the lower plateau potential the

25 polysulfides react with lithium ions and form Li_2S.[23] Therefore, the slight capacity decay was observed the 50th cycle curve, indicating a better reversibility and stability compared with the first cycle. In contrast, the activated carbon-sulfur (AC@S) composite demonstrated a lower capacity, a more negative

30 discharge plateau and a more positive charge plateau after 50 cycles, indicated that the polarization phenomenon of AC@S composite was worse than that of the CSC@S. These results were consistent with the cycling performances shown in Fig. 5a.
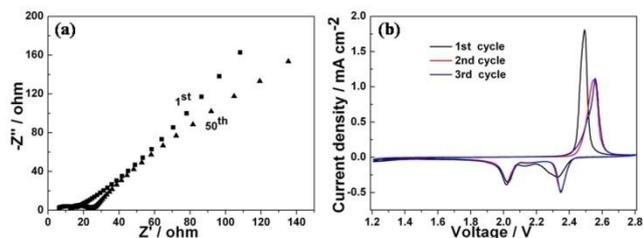
35   **Fig. 6** a) Nyquist plots for electrode of the CSC@S composite, b) cyclic voltammograms of the CSC@S composite based cell in the range of 1.2-2.8 V ($vs.$ Li/Li^{+}) at a rate of 0.05 mV/s.

To further verify the improved electrochemical performance, electrochemical impedance spectroscopy (EIS) was carried out

40 for the CSC@S composite electrodes. Fig. 6a shows the Nyquist plots of the EIS data for the CSC@S composite cells after different cycles. At different cycles the impedance curves exhibit

a semicircle at the high to medium frequency and a nearly straight line at low frequency. The semi-circles relate to the

45 resistances of charge transfer, while, the oblique straight line corresponds to the Li^{+} diffusion process within the cathodes. It is obvious that the CSC@S composite electrode exhibits a low and stable charge transfer resistance during the cycling, which could be attributed to the enhanced conductivity and the stabilized

50 cathode structures.

The first three cyclic voltammetry curves of the CSC@S electrode can be seen in Fig. 6b. Two separated reduction peaks are observed at about 2.05 V and 2.3 V ($vs.$ Li/Li^{+}), and an anodic peak at 2.5 V. In the second cycle, one of the cathodic peaks

55 potential shifts to ~2.35 V, and the anodic peak potential shifts to ~2.55 V, which are ascribed to the polarization of the electrode and indicates the irreversible transform from elemental sulfur to Li_2S_2 or Li_2S.[24-26] After the third cycle, the positions of cathodic and anodic peaks remain almost unchanged, which confirms the

60 good reversibility and stability after the initial electrochemical process in the CSC@S electrode.
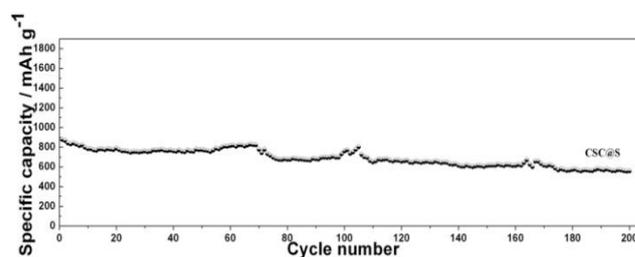
Fig. 7 Long-term cycling performance of the CSC@S cathode at a rate of 0.1 C for 200 cycles.

65 The Li-S battery exhibited a fine cyclability and the reversible capacity stabilizes of ~600 mAh/g was maintained during the test (Fig. 7). After 200 cycles, the cell still delivers a high reversible capacity of 557 mAh/g.

Conclusions

70 In this study, coconut shell based porous carbon with hierarchical pore size was used to fabricate a porous sulfur/carbon composite as the cathode material for lithium–sulfur batteries. The CSC@S composite derived cell reveals excellent cycling stability compared with the cell based on the commercial active carbon.

75 The initial discharge capacity of the cell can be 878 mAh/g at a rate of 0.1 C and remain as high as 774 mAh/g after 50 cycles. Based on the electrochemistry investigations, the porous CSC substrate could prevent the dissolving of the polysulfide into electrolyte. Therefore, the conductivity and structural integrity of

80 cathode could be retained during the cycling, which finally results in the high cycling performance.

Acknowledgements

Notes and references

a *School of Chemistry and Chemical Engineering, Henan Normal University, Xinxiang Henan 453007, China. E-mail: yinyh@163.com; Fax: (+86)-373-3326439; Tel: (+86)-373-3326439*

b *Engineering Technology Research Center of Motive Power and Key*
5 *Materials of Henan Province, Xinxiang Henan 453007, China*
c *Collaborative Innovation Center of Henan Province for Green Motive Power and Key Materials, Henan Normal University, Xinxiang Henan 453007, China*

1   S. Evers and L. F. Nazar, *Accounts Chem Res*, 2013, **46**, 1135.
2   X. L. Cui, Z. Q. Shan, L. Cui and J. H. Tian, *Electrochim Acta*, 2013,
15   **105**, 23.
3   J. B. Goodenough and Y. Kim, *J Power Sources*, 2011, **196**, 6686.
4   A. Manthiram, Y. Z. Fu and Y. S. Su, *Accounts Chem Res*, 2013, **46**,
     1125.
5   D.-W. Wang, Q. Zeng, G. Zhou, L. Yin, F. Li, H.-M. Cheng, I. R.
20   Gentle and G. Q. M. Lu, *Journal of Materials Chemistry A*, 2013, **1**,
     9382.
6   Z. Dong, J. Zhang, X. Zhao, J. Tu, Q. Su and G. Du, *Rsc Adv*, 2013, **3**,
     24914.
7   M.-S. Park, J.-S. Yu, K. J. Kim, G. Jeong, J.-H. Kim, T. Yim, Y.-N.
25   Jo, U. Hwang, S. Kang, T. Woo, H. Kim and Y.-J. Kim, *Rsc Adv*,
     2013, **3**, 11774.
8   W. Wei, J. Wang, L. Zhou, J. Yang, B. Schumann and Y. NuLi,
     Electrochemistry Communications, 2011, **13**, 399.
9   W. Ahn, K. B. Kim, K. N. Jung, K. H. Shin and C. S. Jin, *J Power*
30   *Sources*, 2012, **202**, 394.
10   M. M. Rao, X. Y. Song and E. J. Cairns, *J Power Sources*, 2012, **205**,
     474.
11   S. M. AbstractZhang, Q. Zhang, J. Q. Huang, X. F. Liu, W. C. Zhu,
     M. Q. Zhao, W. Z. Qian and F. Wei, *Part Part Syst Char*, 2013, **30**,
35   158.
12   Z. Wang, X. Niu, J. Xiao, C. Wang, J. Liu and F. Gao, *Rsc Adv*, 2013,
     3, 16775.
13   M. Raoa and X. Songb, *Electrochim Acta*, 2012, **65**, 228.
14   Y. X. Wang, L. Huang, L. C. Sun, S. Y. Xie, G. L. Xu, S. R. Chen, Y.
40   F. Xu, J. T. Li, S. L. Chou, S. X. Dou and S. G. Sun, *J Mater Chem*,
     2012, **22**, 4744.
15   J. Z. Wang, L. Lu, M. Choucair, J. A. Stride, X. Xu and H. K. Liu, *J*
     Power Sources, 2011, **196**, 7030.
16   M. Xiao, M. Huang, S. S. Zeng, D. M. Han, S. J. Wang, L. Y. Sun
45   and Y. Z. Meng, *Rsc Adv*, 2013, **3**, 4914.
17   N. Jayaprakash, J. Shen, S. S. Moganty, A. Corona and L. A. Archer,
     Angewandte Chemie International Edition, 2011, **50**, 5904.
18   X. Ji, K. T. Lee and L. F. Nazar, *Nature Materials*, 2009, **8**, 500.
19   S.-R. Chen, Y.-P. Zhai, G.-L. Xu, Y.-X. Jiang, D.-Y. Zhao, J.-T. Li,
50   L. Huang and S.-G. Sun, *Electrochim Acta*, 2011, **56**, 9549.
20   M. R. Wang, H. M. Zhang, Y. N. Zhang, J. Li, F. X. Zhang and W.
     Hu, *J Solid State Electr*, 2013, **17**, 2243.
21   L. Sun, C. Tian, M. Li, X. Meng, L. Wang, R. Wang, J. Yin and H.
     Fu, *Journal of Materials Chemistry A*, 2013, **1**, 6462.
55 22   H. Ye, Y.-X. Yin, S. Xin and Y.-G. Guo, *Journal of Materials*
     Chemistry A, 2013, **1**, 6602.
23   Y. G. Zhang, Z. Bakenov, Y. Zhao, A. Konarov, T. N. L. Doan, K. E.
     K. Sun, A. Yermukhambetova and P. Chen, *Powder Technol*, 2013,
     235, 248.
60 24   S. Xiong, K. Xie, Y. Diao and X. Hong, *Ionics*, 2012, **18**, 867.
25   Y. Fu and A. Manthiram, *The Journal of Physical Chemistry C*, 2012,
     116, 8910.
26   Y. V. Mikhaylik and J. R. Akridge, *Journal of The Electrochemical*
     Society, 2004, **151**, A1969.

65

Graphic abstract
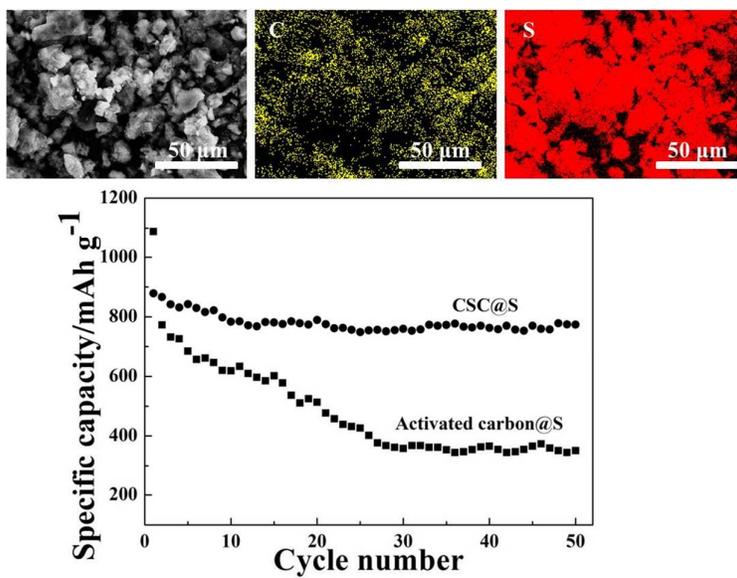
Coconut shells were used as starting material to prepare novel C/S composite for low-cost Li-S battery with high cycling performance.